47th AIAA/ASME/ASCE/AHS/ASC Structures, Structural Dynamics, and Materials Confere
1 - 4 May 2006, Newport, Rhode Island

AIAA 2006-1942

Analysis and Design of Corrugated-Core Sandwich Panels for Thermal Protection Systems of Space Vehicles

Satish K. Bapanapalli[*], Oscar M. Martinez[†], Christian Gogu[‡], Bhavani V. Sankar[§], Raphael T. Haftka[**]
PO Box 116250, University of Florida, Gainesville, FL, 32611-6250

and

Max L. Blosser[††]
Metals and Thermal Structures Branch, NASA Langley Research Center, Hampton, VA, 23681

A preliminary design process of an integral thermal protection system (ITPS) has been presented. Unlike the conventional TPS, the ITPS has both thermal protection as well as load bearing capabilities. The objective of this research work is to establish procedures and identify issues in the design of an ITPS. Corrugated-core sandwich construction has been chosen as a candidate structure for this design problem. An optimization problem was formulated as part of the design process with mass per unit area of the ITPS as the objective function and different functions of the ITPS as constraints. The optimization problem was solved by developing response surface approximations to represent the constraints. Response surface approximations were obtained from finite element (FE) analyses, which include transient heat transfer analyses and buckling analyses. A Matlab code (ITPS Optimizer) has been developed for generating the response surfaces, which has the capability to carry out hundreds of FE analyses, automatically, in conjunction with ABAQUS. Accurate response surface approximations could be obtained for the peak temperatures of the ITPS structure. It was found that response surface approximations for the smallest buckling eigen value of the whole structure were inaccurate. Therefore, the buckling modes were separated and similar buckling modes were grouped together. One response surface approximation was obtained for the smallest buckling eigen value of each group. The preliminary design process for the ITPS generates a design with areal density of approximately 10 lb/ft². Even though the ITPS has much higher load bearing capabilities, it is still on the heavier side when compared to conventional TPS (typical weight 2 lb/ft²). New design changes have been proposed as part of the future work to make the ITPS lighter than the current design.

Nomenclature

θ	=	angle of corrugations
ρ	=	density
d	=	height of the sandwich panel
k	=	thermal conductivity
p	=	half the length a unit cell of the corrugated-core sandwich panel
t_B, t_T, t_W	=	thickness of top face sheet, bottom face sheet and web
C	=	specific heat
M	=	mass per unit area of ITPS panel

---

[*] Graduate Student, Department of Mechanical and Aerospace Engineering, and AIAA Student Member
[†] Graduate Student, Department of Mechanical and Aerospace Engineering
[‡] Graduate Student, Department of Mechanical and Aerospace Engineering
[§] Newton C. Ebaugh Professor, Department of Mechanical and Aerospace Engineering, and AIAA Associate Fellow
[**] Distinguished Professor, Department of Mechanical and Aerospace Engineering, and AIAA Fellow
[††] Aerospace Technologist, NASA Langley Research Center

I. Introduction

WITH the Space Shuttles currently in service due to retire by the end of the decade, it is time to build new vehicles for launching men and material into space. Reusable Launch Vehicles (RLVs), hypersonic military/civilian aircrafts and the Crew Exploration Vehicles (CEVs) require extremely efficient thermal protection systems than the ones currently being used on the Space Shuttles.

NASA plans to send manned missions to Mars in about a decade. In order to slow down space vehicles approaching Mars (or Earth) at hypersonic speeds, aerocapture is a very attractive concept being explored. In this technique, a fast moving space vehicle is allowed to plunge into the planet's atmosphere and the resulting air resistance will provide the necessary braking to slow down the vehicle and put it in orbit around the planet. The aerocapture concept enables a large reduction in the amount of fuel carried by a spacecraft. It can be expected that there would be extremely high aerodynamic heating and pressures due to the air resistance.

The TPS of space vehicles needs to satisfy a wide range of requirements [1-4]. During ascent and reentry, TPS has to withstand temperatures ranging from 377 °C to 1400 °C depending on its position on the vehicle. It is also subjected to aerodynamic pressures. In orbit, the vehicle outer surface may be subjected to cold-soak at temperatures up to -150 °C. Since the TPS forms the outermost surface of the vehicle, it needs to maintain the aerodynamic shape of the vehicle without excessive deformation (thermal bowing and bending due to pressure loads), not be affected by chemical attack such as oxidation, and provide adequate insulation to keep the underlying structure within acceptable temperature limits. It could also be subjected to high speed impact from meteorites, rain, hail, snow, and dust, bird strikes, and lightning strikes. During maintenance and launch preparation, the TPS may be subjected to handling damage, ice buildup, spills of corrosive substances, and low speed impact from rain, hail, and small tools. In order to accommodate all these environments, it is required that the TPS be extremely robust and damage-tolerant and maintain its configuration to effectively perform its primary task of thermal protection.
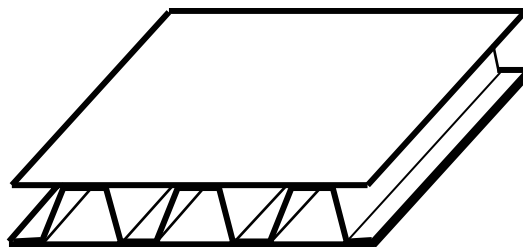
While satisfying all the above requirements, the TPS must also be light weight in order to lower the launch costs. TPS occupies a huge acreage and contributes a significant amount of weight to the spacecraft. The launch cost (for the Space Shuttle) increases by about $10,000 for every pound of launch weight and in order to keep space expeditions economically viable in the 21st century, it is imperative that the launch cost be reduced by an order of magnitude.

The thermal protection systems used on the Space Shuttles are reinforced carbon/carbon (RCC) at the nose and wing leading edges, high and low temperature reusable surface insulation (HRSI, LRSI) used to cover the major portion of the Shuttle windward side, advanced flexible reusable surface insulation (AFRSI) and coated nomex felt reusable surface insulation (FRSI) for the leeward side. While not much can be done with respect to replacing RCC other than develop new materials, there is good scope for developing new structures to replace the LRSI tiles, AFRSI, and FRSI which occupy the major portion on the Shuttle. LRSI tiles are brittle and cannot carry any kind of load (they are separated from the airframe by strain isolation pads, SIPs), as are the AFRSI and FRSI "thermal blankets". These TPS are purely for thermal insulation and protection, while the thermal and pressure loads are borne by the underlying structure.

An attractive alternative for thermal protection is ablation. It may possibly be the only feasible means of thermal protection for Crew Exploration Vehicles (CEVs). Ablative TPS is not a completely reusable TPS. However, if a TPS can be designed such that an ablative component is detachably mounted on a load bearing structure it may be possible to obtain an economical TPS, even if partially reusable. The ablative portion reduces the amount of heat influx into the vehicle, while the load bearing structure carries the aerodynamic pressure loads.

ARMOR TPS, developed by NASA scientists, was an attempt at developing a TPS of fully metallic construction[3]. Metallic TPS are very robust and damage tolerant. Even though the analyses showed that it was very light weight, the design was not suitable for withstanding in-plane loads and large transverse pressure loads. Further, the geometry of the ARMOR TPS was complicated.

Efforts are on to develop Integral Thermal Protection System (ITPS) that not only performs the function of thermal protection, but also withstand loads to a large extent. In a sense, it is an extension of the ARMOR TPS design. One

Figure 1. A typical corrugated-core sandwich structure.

candidate structure suitable for this purpose is a corrugated-core sandwich panel, Figure 1. Sandwich structures have good damage tolerance properties and can withstand small object impact. They are also weight efficient load bearing

structures. Apart from being robust, an ITPS should also be "operable" and easy to manufacture. An operable ITPS is one which can be removed and replaced easily, can be inspected and maintained economically and repaired, when necessary. Corrugated-core sandwich structures are easier to manufacture when compared to truss-core sandwich structures. The manufacturing defects associated with truss-core are not a cause of concern with corrugated-cores. Vacant spaces in between the webs of a corrugated-core can be packed with insulation material (eg., Saffil®) to block the radiation coming from the top face sheet. This is not so easily achievable in a honeycomb sandwich structure. Research has demonstrated that no significant weight savings can be achieved by using a functionally-graded metal foam-core sandwich structures [5]. It is expected that by suitably designing the corrugated-core sandwich structure a robust, operable, weight-efficient, load-bearing TPS can be developed.

The objective of the current research work is to develop techniques to optimize and obtain a minimum mass corrugated-core sandwich structure to function as an integral thermal protection system (ITPS) for space vehicles. The design process for the corrugated-core ITPS was started by simplifying the geometry of the panel so as to include a minimum number of geometric (design) variables. Even in the early stages of design, it was evident that this particular design would not be a useful final design. However, the reduced number of design variables provided an opportunity to establish a design procedure, which can subsequently be used for more complicated designs with a larger number of variables. Further, this optimized design is useful in obtaining an approximate starting design for further design refinements.

The design process was formulated as an optimization problem with mass per unit area of the ITPS being the objective function. The various functional requirements of the ITPS were formulated as constraints of the optimization problem. Each of these constraints was obtained as a response surface approximation, which is a function of the design variables. These response surface approximations were determined by carrying out finite element analysis for different combinations of design variables. Accurate response surface approximations could be obtained for the peak temperatures of the ITPS structure. It was found that response surface approximations for the smallest eigen value of the whole structure were inaccurate. In order to obtain accurate approximations, the buckling modes were separated and similar buckling modes were grouped together. One response surface approximation was obtained for the smallest buckling eigen value of each group. These approximations were found to be fairly accurate for the preliminary design process.

This manuscript contains a detailed description of the ITPS design process using finite element analysis of a simplified ITPS structure. First, the simplified geometry is presented and the geometric variables are listed. Then the optimization problem for the ITPS design is stated. This is followed by a detailed description of the finite element analyses for transient heat transfer and buckling. Then the procedure for response surface generation is presented along with a description of a Matlab code (ITPS Optimizer) used for response surface generation. Finally, the optimization procedure is presented followed by a discussion on the optimized designs.

II. Simplified Geometry and The Optimization Problem

The simplified geometry of the ITPS structure is shown in Figure 2. This geometry can be completely described using the following 6 geometric variables:

1. Thickness of top face sheet, t_T,
2. Thickness of bottom face sheet, t_B,
3. Thickness of webs, t_W,
4. Angle of corrugations, θ,
5. Height of the sandwich panel (center-to-center distance between top and bottom face sheets), d,
6. Length of a unit-cell of the sandwich panel, $2p$.

It should be noted that in, simplifying the design, the corrugated-core has been modified to a structure made of discrete webs not attached to one another by horizontal sections (compare with Figure 1). The horizontal sections of the corrugated-core provide a variety of options with which to efficiently join the core to the face sheets. However, from a design point of view, these sections are redundant. The horizontal sections of the core are, therefore, ignored in the preliminary design.

The design process for the ITPS can be formulated as an optimization problem. The objective is to make the structure as light as possible while fulfilling all the functions required of an ITPS. Therefore, the obvious choice for an objective function would be mass per unit area of the ITPS panel, M, also known as *areal density*. Various functions of an ITPS panel can be formulated in the form of constraints for the optimization problem. Thus the objective of the optimization problem would be to minimize the areal density of the panel while satisfying all the

constraints such as temperature, stress and deflection limits in various parts of the structure, and global/local buckling limits.

Critical functions of an ITPS that would influence its design were taken into account [3]. The following are the four critical constraints taken into account for the preliminary design:

1. Maximum temperature of the bottom surface of the panel must be below certain limit.
2. Panel must be able to withstand global/local buckling due to mechanical and thermal forces.
3. Maximum stresses in the various members of the panel must be within allowable limits.
4. Maximum deflection of the top surface of the panel must be below acceptable limit.

ITPS panels form the outer skin of the vehicle, which encompasses the crew compartment (CEVs) or liquid fuel tanks (X-33-like design). The temperature of the bottom surface determines the amount of heat flowing into the vehicle interiors. Thus, peak bottom surface temperature is an important design driver. While peak temperature of any part of the ITPS panel should be within allowable limits, why is only the peak bottom surface temperature considered critical? Initial heat transfer analyses had indicated that the peak temperature of the top surface is always close to the radiation equilibrium temperature. It is determined by the emissivity of the top surface, which typically has a value of 0.8 to 0.85 [3]. Increasing the emissivity is a manufacturing and material selection issue and not a design issue. The amount of heat entering the vehicle can be decreased considerably by decreasing the heat

Figure 2. A unit-cell of the simplified ITPS design. *The six variables describing the geometry are illustrated. Directions y- and z- of the global coordinates system of the ITPS panel are also shown (x-axis comes out perpendicular to the plane of the paper. The s-axis is part of a local coordinate system for the webs.*

conduction path. This will increase the top surface temperature slightly. However, this increase in temperature is small, typically of the order of 20 K. Thus, the top surface temperature is not a quantity that can be significantly influenced by changing the ITPS design. It is determined by the radiation equilibrium temperature, which is determined by the incident heat flux on the vehicle and the emissivity of the top surface. Thus, the temperature of the rest of the structure is dictated by the temperature limit imposed on the bottom face sheet.
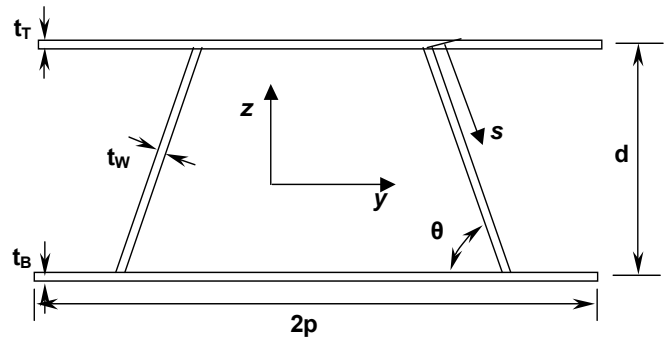
When the whole ITPS panel buckles as a plate, it is referred to as global buckling. When the buckling is limited to a part of the panel, such as one of the webs or a section of the face sheets, then it is referred to as local buckling. Global buckling may not be a factor in the ITPS design because the ITPS panel is expected to be a thick panel. However, local buckling can be a major design driver because the ITPS structure is made of thin plates, which are susceptible to buckling.

In the case of maximum allowable stress constraint, it should be noted that some parts of the structure are at very high temperatures and temperature dependence of material properties, like yield stress and Young's modulus should be taken into account to obtain correct stresses.

Limits on the deflection of the top surface are imposed because excessive deflection of the top surface could lead to extremely high local aerodynamic heating [1]. Due to heat input, the temperature of the whole panel increases. Some of the heat is transferred to the stringers and frames of the vehicle and the whole vehicle grows in size. This overall deflection is not of a major concern, as it does not change the aerodynamic profile of the vehicle significantly. However, local deflections, such as face sheet dimpling, can lead to severe local aerodynamic heating. Therefore, when the limit on top surface deflection is imposed, the overall increase in size of the vehicle should be deducted.

III.   Finite Element Analysis for Heat Transfer

This section deals with the details of the finite element analysis used to solve the heat transfer problem of the ITPS. It will help determine the peak bottom face sheet temperature, which is required for the temperature constraint, and will provide the temperature distribution in the panel that can be used for buckling, stress and deflection constraints.

A. Incident Heat Flux

Incident heat flux on the vehicle depends on the shape of the vehicle, the trajectories of the ascent and reentry and is completely different for vehicle ascent and reentry conditions. For the preliminary design process, incident heat flux of a Space Shuttle-like vehicle is used.

Figure 3A shows the heat flux input for ascent conditions, while Figures 3B and 3C show the heat flux during reentry on the windward and leeward centerlines of the vehicle respectively, obtained from Ref 1. The heating profiles for windward and leeward sides are similar during ascent [1]. Windward centerline is a line drawn on the vehicle surface connecting the nose to tail on the topside of the vehicle, while leeward centerline joins the nose and tail on the bottom side. Different curves on each figure are for heating rates at different points along the centerlines. The distance x, on the charts, indicates the distance from the nose tip of the vehicle, which implies that $x = 0.0$ inches represents the nose-tip of the vehicle. The heating rates are extremely high for points closer to the nose of the vehicle. Comparing Figures 3A and 3B, it is quite obvious that the reentry heating rates are more severe than the heating rates during ascent, that is, the heating rates increase more steeply and the total integrated heat load is much larger during reentry. Thus, it can be inferred that the reentry heating rates would be most influential in designing the ITPS and these heating rates were considered for heat transfer FE analysis.

The heating rate used for preliminary design is shown in Figure 4, which corresponds to a point, $x = 827$ inches [3]. Peak radiation equilibrium temperature for this heating profile is 968 K.
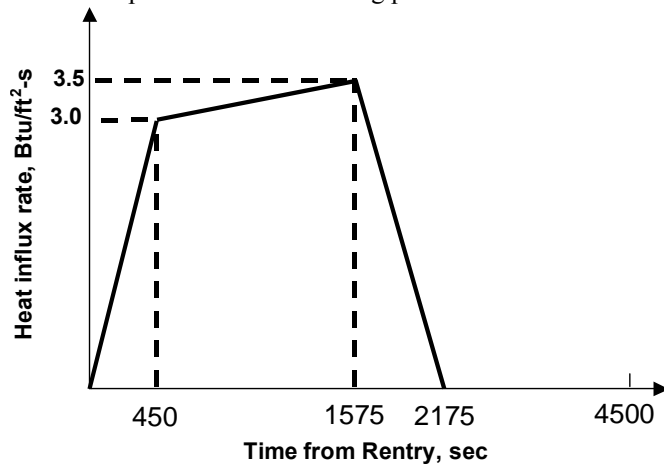

Figure 3. **Heating profiles for a Shuttle-like vehicle obtained from Ref [2].** *A) during ascent on vehicle windward centerline, B) during reentry on vehicle windward centerline, C) during reentry on vehicle leeward centerline.*

Figure 4. **Heating profile used for preliminary design of ITPS**

B. Boundary Conditions and Load Steps

Loads and boundary conditions imposed on the structure in the FE analysis are schematically illustrated in Figure 5. Initial temperature of the structure is assumed to be 295 K (72 F). Heat flux is incident on the top surface of the top face sheet. A large portion of this heat is radiated out to the ambient by the top surface. The remaining heat is conducted into the ITPS. Some part of this heat is conducted to the bottom face sheet by the insulation material and some by the webs. The bottom surface of the bottom face sheet was assumed to be perfectly insulated. This is a worst-case scenario where the bottom face sheet temperature would rise to a maximum as it cannot dissipate the heat. The optimization with this assumption
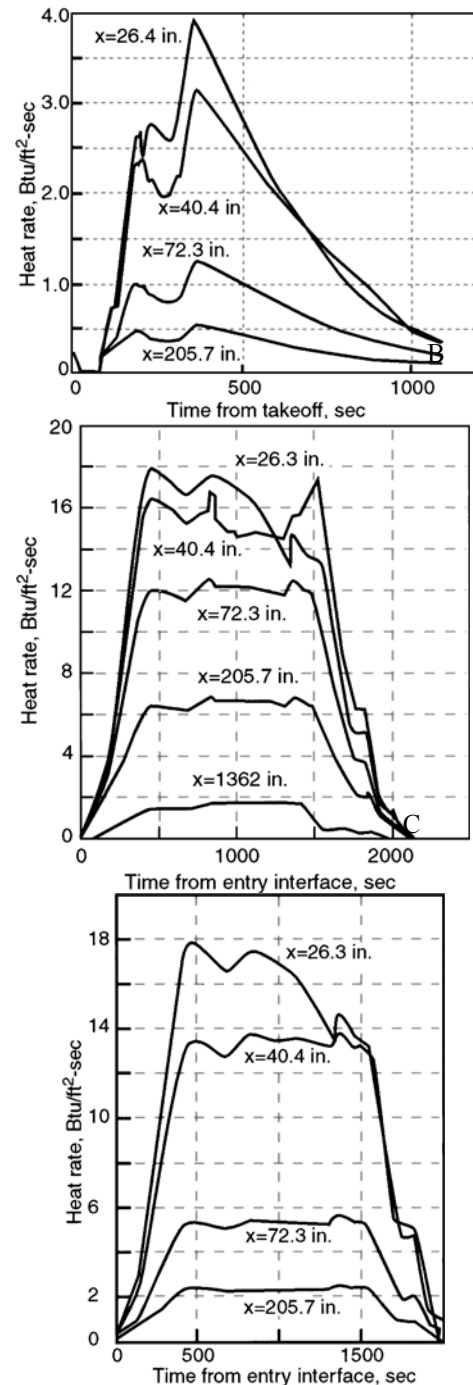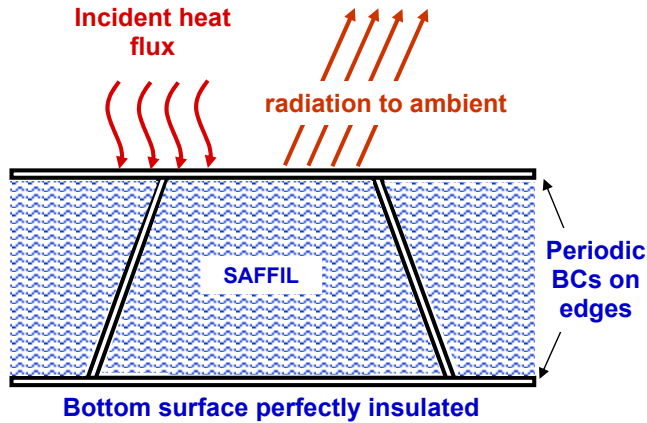
Figure 5. Loading and boundary conditions for the heat transfer problem.

would lead to a conservative design. It is also assumed that there is no lateral heat flow out of the unit cell, that is, the heat flux incident on a unit cell is completely absorbed by that unit cell only. In an actual ITPS panel, the heat would flow into the stringers and frames and there would be a lateral flow of heat in the panel from one unit cell to another. The temperature distribution could be completely different in case of heat flowing out of the unit cell. This is not taken into account in the preliminary design.

Ambient temperatures are assumed to be 213 K for initial reentry period (0 to 450 seconds), 243 K for the second reentry phase when heating rate remains approximately constant (450 to 1575 seconds), and 273 K for the final phase of reentry (1575 to 2175 seconds). Initial heat transfer analyses indicate the peak bottom face sheet temperature occurs after vehicle touchdown [3]. After touchdown the FE analysis continues for another 30 – 45 minutes to capture the temperature rise of the bottom face sheet. During this period, along with radiative heat transfer, convective heat transfer boundary conditions are imposed on the top surface to simulate the heat transfer to the surroundings while the vehicle is sitting on the runway. The value of convective heat transfer coefficient, h, used was 6.5 W/m^2-K (6.94×10^{-4} Btu/s-ft^2-°R) [3]. The ambient temperature during this period is assumed to be 295 K.

The transient heat transfer analysis is divided into 4 load steps as shown in Table 2. Step 1 ranges simulates the initial reentry phase, when the heating rate is linearly ramped up from 0 to 3.0 Btu/ft^2.sec, Step 2 simulates the second phase of reentry, when the heating rate is linearly ramped up from 3.0 to 3.5 Btu/ft^2.sec, and Step 3 simulates the final phase of reentry, when the heating rate is ramped down from 3.5 to 0.0 Btu/ft^2.sec. During these load steps, the top surface has incident heat flux loading and radiation boundary conditions. Step 4 simulates the phase after vehicle touchdown. There is no heat input during Step 4 and the top surface has radiation and convective heat transfer boundary conditions.

Other assumptions of note include an assumption of a perfect conduction interface between the face sheets (and webs) and the insulation materials, that is, there is no thermal contact resistance at the interface. The insulation material is usually made of a low density porous material, such as SAFFIL, which is made of alumina fibers. Even though this insulation material is assumed to completely block out all the radiation from the top surface to other parts of the ITPS, there is some radiative heat transfer to the interior of the ITPS due to the porous nature of the insulation material [1,4,5]. Also, there could be a convective heat transfer through the insulation material due to the gases present in the pores [1,4,5]. For the preliminary design process, radiative and convective heat transfer through the insulation material is ignored and only the conductive heat transfer is taken into account.

Load Step	Time Period	Heat Flux Input	Time Step Size	Ambient Temperature
STEP 1	0 – 450 sec	0.0 – 3.0 Btu/ft^2.sec Ramp linearly	15 sec	213 K
STEP 2	450 –1575 sec	3.0 – 3.5 Btu/ft^2.sec Ramp linearly	15 sec	243 K
STEP 3	1575 –2175 sec	3.5 – 0.0 Btu/ft^2.sec Ramp linearly	15 sec	273 K
STEP 4	2175 –5175 sec	-	40 sec	295 K

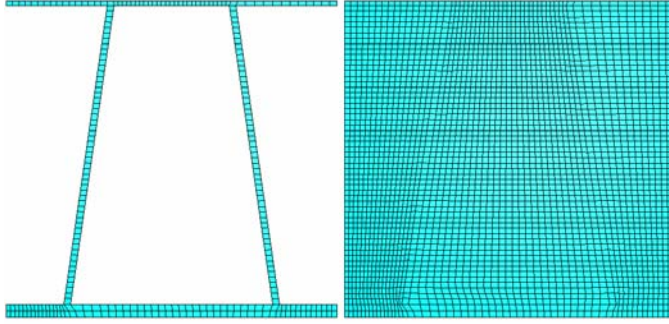**Table 1.   Load steps in the FE heat transfer analysis.**

C. One-Dimensional and Two-Dimensional FE Models

As explained in the previous section, there is no lateral heat flow across the unit cells. Thus, the FE heat transfer analyses is limited to one unit cell instead of modeling the whole ITPS panel. Further, a 2-d FE model in the *y-z* plane (refer Figure 2 for the coordinate directions) is sufficient as there would be no temperature variation in the *x*-direction in this design. The heat transfer FE problem could be further simplified to a 1-d model. This would considerable reduce the analysis time for the transient heat transfer analysis. In order to show that a 1-d model can

effectively do the job of a 2-d model, a comparative study was carried out. All finite element analyses for this research were carried out using ABAQUS finite element software package.

A typical 2-d FE model is shown along with its mesh in Figure 6. The solid portion of the ITPS is made of titanium alloy (Figure 6A) and the insulation material is Saffil. Temperature dependent material properties were used for both materials. Eight-node quadrilateral heat transfer element is used for 2-d modeling (ABAQUS element DC2D8). 10149 nodes and 3306 elements were used for this model.

Figure 6. Typical mesh for 2-d heat transfer problem *A) the solid portion of ITPS only, B) complete ITPS including the insulation material in between the webs.*

face sheet thicknesses. One-dimensional 3-node heat transfer link element (ABAQUS element DC1D3) was used for this model. 109 nodes and 54 link elements were used in this model. Figure 7 schematically illustrates the 1-d model. The corrugated-core of the panel is homogenized, while the top and bottom face sheets remain the same as in the 2-d model. The homogenized properties of the core are calculated by the rule of mixtures formulae. The formulae below show the homogenized properties for density, specific heat and thermal conductivity.

A 1-d FE heat transfer model is just a straight line of length equal to the height of the ITPS panel plus the top and bottom

Homogenized Core = SAFFIL + Ti

Figure 7. One-dimensional heat transfer model representation.

$$\rho^* = \frac{\rho_1 V_1 + \rho_2 V_2}{V^*} \tag{1}$$

$$C^* = \frac{C_1 \rho_1 V_1 + C_2 \rho_2 V_2}{\rho^* V^*} \tag{2}$$

$$k^* = \frac{k_1 A_1 + k_2 A_2}{A^*} \tag{3}$$

ρ stands for density, C for specific heat, and k for conductivity. The subscripts 1 and 2 represent titanium and SAFFIL, respectively, while the superscript * represents the homogenized core. A stands for area of cross-section through which the heat flows where A_1 is given by the formula shown below, which takes into account the angle of corrugations, θ.

$$A_1 = \frac{2t_w}{\sin\theta} \cdot 2p \tag{5}$$

Figure 8 shows the comparison between the 1-d and 2-d FE heat transfer analyses results for an ITPS panel. Heat flux input, boundary conditions and materials selection were imposed as discussed in the previous section. Figure 8A shows the temperature versus reentry time for two locations on the 2-d model. Loc-1 and Loc-2 are two points on the top face sheet (shown in the inset on Figure 8A) where the temperatures are at the extremes. The 1-d heat transfer analysis does a good job of predicting the top face sheet temperature, which is approximately the average of the temperatures at Loc-1 and Loc-2 in the 2-d model.
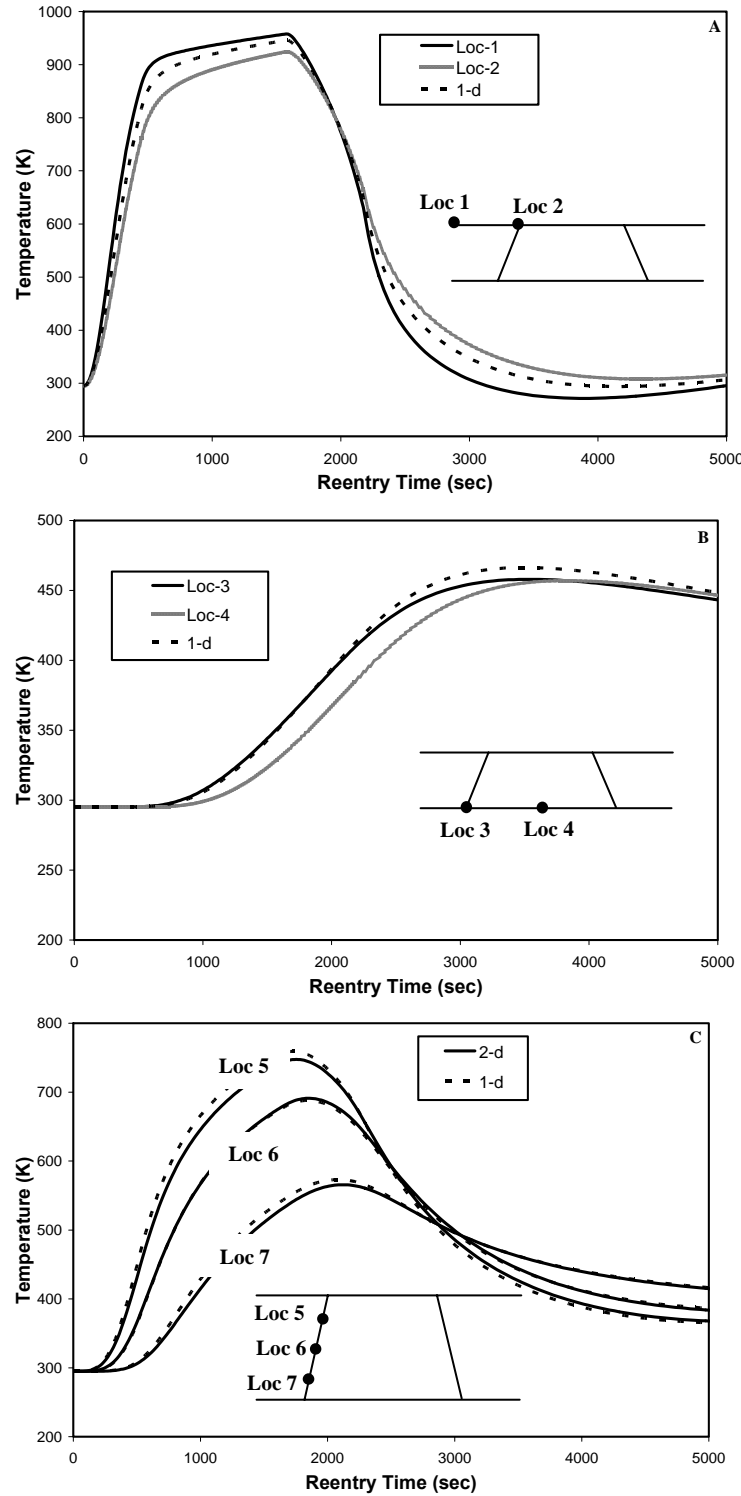
Figure 8. Comparison of 1-d and 2-d heat transfer analyses, *with dimensions $t_T = 2.0$ mm, $t_B = 6.0$ mm, $t_W = 3.0$, $\theta = 82.0$, $d = 140$ mm, $p = 75$ mm, A) top face sheet temperatures, B) bottom face sheet temperatures, C) Web temperatures.*

Figure 8B shows the temperature variation with time on the bottom face sheet. Loc-3 and Loc-4 are two of the extreme locations (shown in the inset on Figure 8B) on the bottom face sheet. The predictions of the 1-d model in this case are slightly higher than the 2-d model temperatures. The maximum difference is around 5%, which can be ignored for the preliminary design. Figure 8C shows the temperature variations at 3 different locations on the web. The 1-d model does a very good job of predicting the temperatures at all these locations. An important conclusion from Figure 8C is that the 1-d model does a good job of predicting the temperature distribution through the thickness of the ITPS panel. Thus, it can be concluded that the 1-d heat transfer finite element computes the temperatures and temperature distributions sufficiently accurately at all reentry times and can be reliably used for the design process.

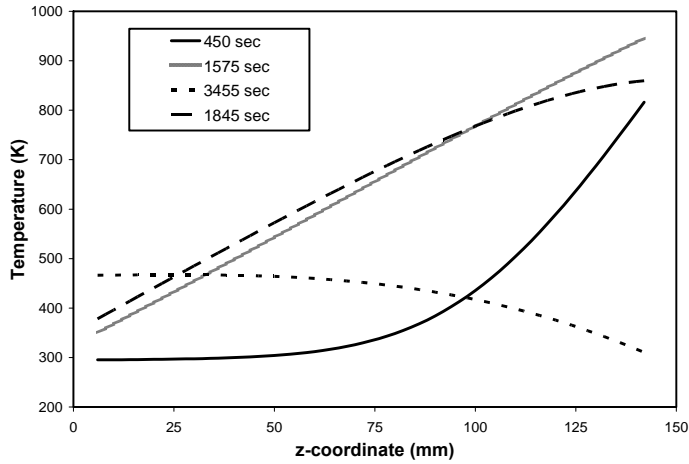## D. Temperature vs. Reentry Time and Temperature Distribution

Temperatures vs. reentry time curves for top and bottom face sheets, and mid point of web are shown in Figure 9 for comparison purposes. The dimensions of the ITPS used here are same as those shown in Figure 8. As mentioned earlier, the temperature on the bottom surface peaks after the vehicle landing (approximately 2175 sec). These curves were obtained from the 1-d heat transfer analysis.

Temperature distributions through the thickness of the ITPS panel are shown in figure 10 for different reentry times. At 1575 seconds the top surface reaches its peak temperature, at 3455 seconds the bottom surface reaches its maximum temperature and at 1845 seconds the mid point of the web reaches its maximum temperature. The distribution is non-linear as expected. Each of these temperature distributions can be accurately represented by a complete cubic polynomial in one variable (z-coordinate) obtained using least squares approximation.
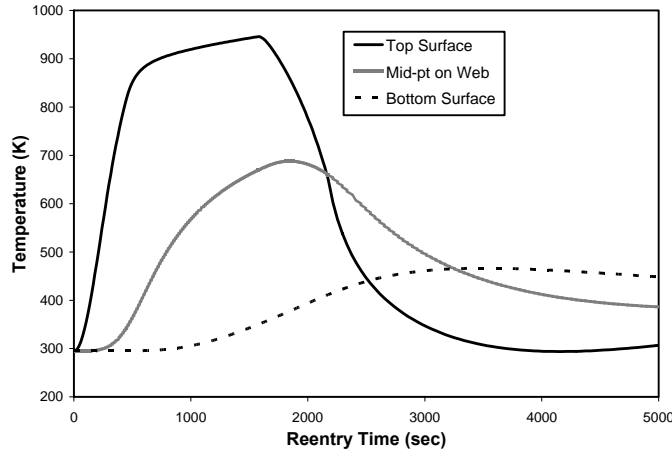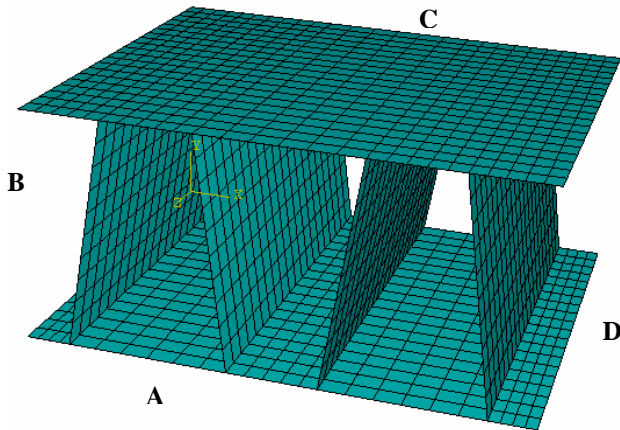
Figure 9. Temperature variation vs. reentry times for top and bottom surfaces and web mid-point obtained from 1-d heat transfer analysis. *Dimensions of the ITPS are the same as listed in Figure 8.*

Figure 10. Temperature distribution through the thickness of the ITPS panel at different reentry times. *Dimensions of the ITPS are the same as listed in Figure 8.*

Figure 11. Typical FE shell element mesh for buckling analysis. Two unit cells are shown in this figure. The panel edges are marked A, B, C and D.

IV. Finite Element Buckling Analysis

The ITPS panel is to be designed to withstand significant transverse mechanical loads and extreme thermal gradients. In order to make the ITPS economical, it is necessary to design panels which are large in size. This would imply that there would be large unsupported or partially supported sections of thin plates (face sheets, webs) subjected to various kinds of loads including thermal compressive stresses and in-plane mechanical compressive loads. Such sections would be susceptible to buckling. Local buckling, by itself, may not always lead to catastrophic failure. However, it could contribute to failure, indirectly. For example, if the top surface buckles locally it could lead to extremely high local aerodynamic heating, which could prove to be catastrophic.

Finite element analysis for buckling is carried out using ABAQUS. In the finite element model, only the solid portion of the ITPS panel is taken into account, which includes the face sheets and the web. The insulation material is not considered to be a structural member. This is indeed true because Saffil insulation is a soft fibrous insulation with hardly any mechanical properties when compared to the properties of the solid material that make up the webs and face sheets. Therefore, it can be safely omitted from all structural analyses without introducing any palpable error.

The ITPS panel is made of thin plates. Therefore, 3-d shell element is the most suitable element for modeling the structure. Eight-node shell element (ABAQUS element S8R) with 6 degrees of freedom at each node (3 displacements and 3 rotations) and reduced integration was used for the buckling FE model. Around 5560 nodes and 1820 elements were used for each buckling model.

In the heat transfer problem a unit-cell analysis was carried out. Unit-cell analysis is not possible for the buckling problem because the boundary conditions for a unit-cell buckling problem are unknown. Therefore, the buckling analysis was carried out by including the whole ITPS panel in the FE model. Figure 11 shows one-quarter of an ITPS panel. The panel has a total of 4 unit cells. Only 2 unit cells are necessary to model the ITPS panel by taking into account the symmetry of the panel. In this model the boundary conditions at the panel edges can be imposed as discussed below. This

introduces an additional variable into the problem, which is the length of the panel (considering only square shaped panels). Instead of the length, the number of unit-cells in the panel could be considered as a variable. For preliminary design, the number of unit cells was fixed at 4 per panel. Therefore, by changing the length of the unit-cell, *2p*, the length of the panel can be changed. Thus the number of variables still remains at 6.

The loads for the buckling problem are temperature loads and aerodynamic pressure loads. Temperature distributions are obtained from the heat transfer problem at different reentry times in the form of complete cubic polynomials in one variable (z-coordinate). Using these polynomials the temperatures are assigned to each node of the 3-d shell mesh according to the z-coordinates of the nodes. In this way the temperature load is imposed for the buckling problem. Note that the buckling problem is separate for each reentry time. If 4 different reentry times are chosen, then there are 4 different buckling problems with 4 different temperature distributions. One notable approximation introduced here is that the face sheet temperatures are uniform throughout their respective lengths and widths. This is because the temperature distribution is a function of only the z-coordinate of the nodes. Considering the magnitude of temperature variation on the face sheets, this is a minor approximation. The aerodynamic pressure load on the vehicle during reentry is shown in Figure 12. It was assumed that the internal pressure of the vehicle is equal to the atmospheric pressure. Therefore, a net pressure load of 1 atm (101325 Pa)
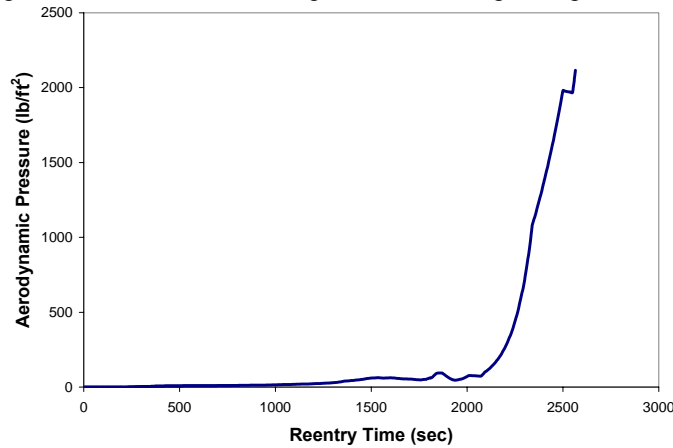
Figure 12. Aerodynamic pressure load on the TPS. *The pressure remains close to zero during the entire reentry phase and become equal to the atmospheric pressure after landing.*

would be acting on the inner surface of the top face sheet.

For the ITPS buckling problem, the FE analysis is divided into two steps. Step 1 corresponds to the base state. In this state all the boundary conditions and the "non-critical" loads are imposed. In Step 2 (eigenvalue step), the critical loads are imposed. For the ITPS problem for a Shuttle like design, aerodynamic pressure load can be considered non-critical load while the thermal stresses caused by the temperature loads can be considered to be a critical load. The definition of critical and non-critical loads can be altered according to the problem. For example, in the ITPS design for a CEV, there will be tremendous dynamic pressure loads on the ITPS and this could be a more critical load than the temperature loads.

The boundary conditions on the ITPS panel are dependent upon how the panels would be mounted on vehicle. For this research, it is assumed that the edges of the panels are mounted on the stringers and frames of the vehicle. Usually, provision is made for the panels to expand slightly when heated. This arrangement precludes the development of large thermal stresses. The top face sheet experiences the highest temperatures and should be allowed to expand as much as possible. For preliminary design analysis it is assumed that the edges of the bottom face sheet of the panels are mounted on the stringers and frames with a provision to expand freely in plane while restricting the out of plane motion and all the rotations on the edges. The edges of the top face sheet are fixed with respect to all 3 rotations while allowing the displacements.

In the FE buckling analysis, only one quarter of the panel was modeled by taking advantage of the symmetry conditions. Since the number of unit-cells was fixed at 4 per panel, only 2 will appear in the FE model. Figure 11 shows the 2 unit cells and the FE mesh. On Edge A and Edge B, which are the actual panel edges, the bottom face sheet edges were fixed in z-direction displacement and all three rotations, and the top face sheet edges were fixed in all three rotations while allowing all three displacements. Edges C and D are the symmetric edges in the FE model. On Edge C, the top and bottom face sheet symmetric edges and the web symmetric edges were fixed in *x*-direction displacement and *y*- and *z*-direction rotations to simulate the symmetry boundary conditions. Similarly, the symmetry boundary conditions on Edge D were simulated by fixing the *y*-direction displacement and *x*- and *z*-direction rotations.

In ABAQUS buckling eigen value problem, desired number of eigen values can be specified. For example, if 40 eigen values are desired, then ABAQUS extracts 40 smallest eigen values and eigenvectors. The reason for obtaining 40 eigen values is because in some cases the first few smallest eigen values are negative values. These negative eigen values are for cases where the load is applied in the opposite direction compared to the current loads. The negative eigen values do not make sense for the current design procedure and are ignored. An eigen value 0.7 implies that at 70% of the applied load the structure would buckle according to the corresponding buckling mode. If the smallest eigen value is above unity, then the structure will not buckle under the applied loads. The 40

eigenvectors (buckling modes) can also be obtained in the form of nodal displacements. The eigenvectors are normalized such that the maximum displacement is equal to unity. By determining the position of the node, at which the displacement is equal to unity, the buckling mode can be identified.

V. Response Surfaces

For the current ITPS design problem, a quadratic response surface approximation of each constraint was adopted to solve the optimization problem. The response surface approximations are functions of design variables. The procedure for obtaining the response surface approximations is outlined below.

A quadratic response surface approximation in 6 variables has 28 coefficient and hence at least 28 function evaluations are required. Usually the number of function evaluations, N, required for obtaining a fairly accurate response surface is twice the number of coefficient. For preliminary design, N has been typically found to be greater than 100 in order to obtain sufficiently accurate response surfaces. Latin Hypercube Sampling (LHS) is used for the design of experiments. A range has to be specified for each variable. The Latin Hypercube scheme divides each of these ranges into N equally spaced intervals. Then it randomly picks one value within each of these N intervals. An optimized LHS technique was used where the minimum distance between the picked variables is maximized. This scheme ensures that while there is some randomness in picking up the variables, the variables are not clustered in any region of their respective ranges, but are fairly equally distributed across the whole range. The N values per variable are then randomly combined to form N experiments.

Using each of these N combinations of geometric variables, N heat transfer finite element analyses can be carried out. The maximum bottom face sheet temperature for each of these N experiments is obtained from the analyses. Thus we obtain N function values for N different combinations of the variables. Using these function values and combinations of variables, a complete quadratic polynomial in 6 variables can be obtained by the Least Squares Approximation (LSA) method. This polynomial is the response surface approximation for the peak bottom face sheet temperature. The approximation can be used to obtain peak bottom face sheet temperature for any combination of variables with each variable chosen from its respective range. In solving the optimization problem, the temperature constraint can be imposed using this response surface, such that the peak bottom face sheet temperature is below certain limit, say 200 °C. Response surfaces obtained using LSA method cannot be guaranteed to be accurate if a variable value is chosen outside its range.

For buckling problem the response surfaces are obtained for the smallest buckling eigen values. The buckling analysis is carried out at different reentry times. This is because the temperature distribution is completely different for different reentry times and therefore the buckling modes would also be very different at different times. For preliminary design, the following 4 "critical" reentry times were chosen to carry out the buckling analyses:

1. 750 seconds (Time 1),
2. Time when top face sheet reaches maximum temperature (Time 2),
3. Time when bottom face sheet reaches maximum temperature (Time 3), and
4. Time when mid-point of the web reaches maximum temperature (Time 4).

Times 2 to 4 are obvious choices because peak temperatures usually correspond to peak stresses. Time 1 is considered critical because it was observed that around 750 seconds, the temperature of the bottom face sheet is, usually, still at its initial temperature value. This can be considered to be approximately the time at which the temperature gradient is most severe in the structure.

The same design of experiments used for heat transfer analysis is used for the buckling analysis. Using the combinations of variables obtained by optimized Latin Hypercube Sampling, the 3-D FE model for buckling is created. Temperature distributions at Times 1, 2, 3 and 4 are obtained from the heat transfer analysis. The temperature distributions are imposed on the nodes of the 3-D FE buckling mesh, and first 40 smallest eigen values are obtained for each buckling analysis. From these values the smallest positive eigen value is obtained for each temperature distribution. Thus, 4 eigen values are obtained for each combination of geometric variables, each corresponding to one of the critical reentry times. Using the smallest eigen values as function values, 4 different quadratic response surfaces are obtained by the LSA method. Each response surface gives the smallest eigen value at one of the 4 reentry times. Thus, the buckling constraint (Constraint 2) has been split into 4 constraints. The response surfaces can be used to impose the buckling constraint such that the smallest eigen value at each of these reentry times is greater than unity. If a factor of safety is desired then the eigen value limit can be increased to 1.5 for a 50% factor of safety, for instance.

Theoretically, the number of possible buckling modes is equal to the number of degrees of freedom in the FE analysis. Depending upon the geometry of the structure, the first buckling mode can be different for different experiments even for the same reentry time or temperature distribution. Therefore, initial attempts at obtaining the response surfaces for smallest eigen values produced highly erroneous results. The response surfaces did a very poor job at predicting the smallest eigen value for different combinations of geometric variables.

In order to decrease the error and make the response surfaces more accurate, the buckling modes were further subdivided. At each reentry time, the smallest eigen value for top face sheet buckling, bottom face sheet buckling and web buckling were obtained separately. Response surfaces for each of these eigen values were again obtained using LSA method. Therefore, for each reentry time there are 3 response surfaces. For 4 reentry times, there would be a total of 12 buckling response surfaces.

In all, a total of 13 response surfaces can be generated as listed below:

- One response surface for maximum bottom face sheet temperature,

- Four response surfaces for smallest bottom face sheet buckling eigen value at Times 1, 2, 3 and 4,

- Four response surfaces for smallest top face sheet buckling eigen value at Times 1, 2, 3 and 4,

- Four response surfaces for smallest web buckling eigen value at Times 1, 2, 3 and 4.

The procedure to generate these response surfaces from FE experiments' results will be discussed in the following section.

## VI.   Response Surfaces Generation: ITPS Optimizer

Typically, it has been found that 100 function evaluations give sufficiently accurate response surfaces. This would imply that 100 heat transfer FE analyses plus 100×4 FE buckling analyses need to be carried out. The number of required function evaluations could be as high as 150 if the ranges of the variables are large. Further, the process has to be repeated whenever there is a small design change. This is a formidable number of FE analyses and it is improbable to be carried out manually.

A Matlab code has been developed for this purpose called the *ITPS Optimizer*. This program activates ABAQUS through Matlab and performs the FE heat transfer and buckling analyses automatically. The functions of ITPS Optimizer are illustrated by the flowchart in Figure 13.

The ITPS Optimizer first obtains a design of experiments using Latin Hypercube Sampling. It carries out the FE heat transfer and buckling analyses for one combination of variables at a time. First the geometric variables are used to create a 1-d heat transfer ABAQUS model using ABAQUS scripting commands. An input file is obtained from the model and modified to include the radiation and convection boundary conditions. The input file is executed by the ABAQUS Standard Solver to obtain an Output Database (ODB) file, which contains the solution to the heat transfer finite element analysis. Using Scripting Commands, temperature versus time and nodal temperature data is obtained from the ODB file. This data is then processed to determine the maximum bottom face sheet temperature and the temperature distributions at the 4 different reentry times. The bottom face sheet temperature is printed out to results file, while the temperature distributions are carried forward for buckling analysis.

A 3-d buckling ABAQUS model is created using the Scripting commands and the geometric data from the design of experiments. An input file is then generated that contains all the data relating to geometry, material property and boundary conditions. Using this input file, 4 new input files are created by imposing the nodal temperature loads from the temperature distributions obtained from the heat transfer analysis. These input files can then be suitably used to carry out buckling analysis and linear stress analysis. From the buckling ODB files, the smallest buckling eigen values are obtained. From linear stress analysis ODB files stresses in different ITPS sections and top face sheet deflections can be extracted. The details of linear stress analysis have not been presented in this manuscript because the stresses and deflections were not critical to the preliminary design. However, the ITPS Optimizer has the capability for linear stress analysis and this might be useful in future designs.

In the flow chart (Figure 13) the ouput from the ITPS Optimizer is listed in the ellipses on the right hand side. This data is obtained for all the experiments and then used to determine the 13 response surfaces for temperature and buckling.
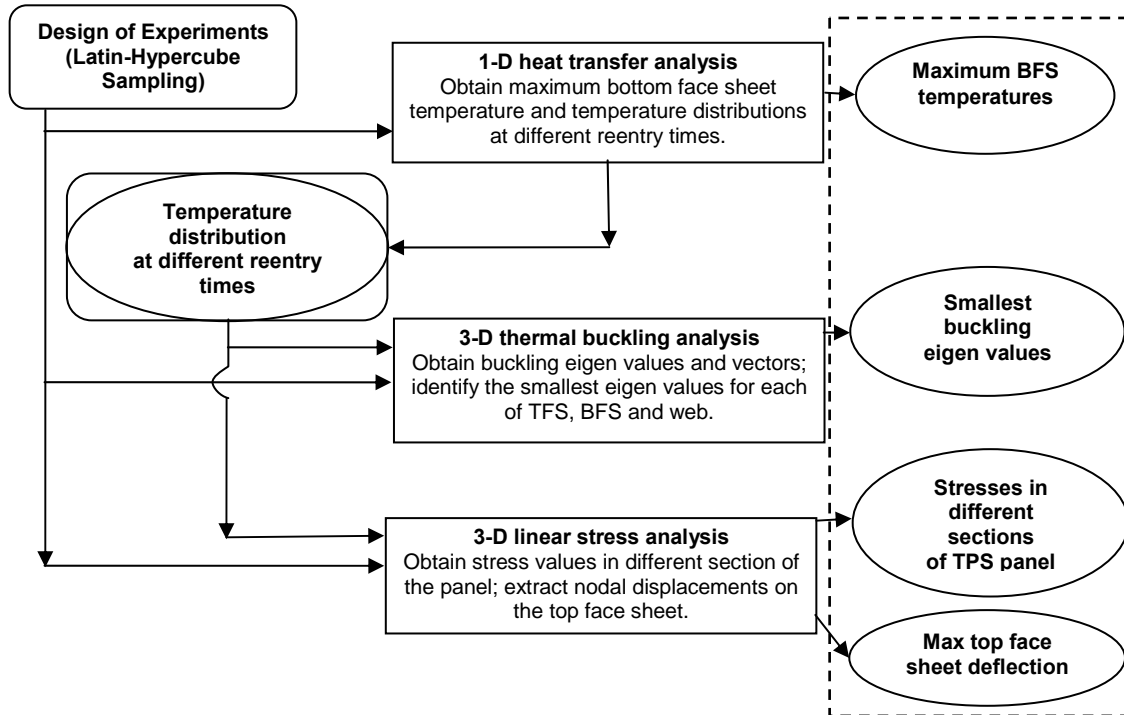
Figure 13. Flowchart illustrating the procedure followed by the ITPS Optimizer. *Rounded boxes represent inputs for FE analyses, rectangles for FE analyses and ellispses represent FE output. Temperature distributions are output of heat transfer analysis and input for buckling and linear stress analysis. The dotted rectangle containing the ellipses represents the data output from ITPS Optimizer, which is used for generating response surface approximations.*

VII.   Optimization and Optimized Design

The heating rate chosen for preliminary design is shown in Figure 4. The peak radiation equilibrium temperature for this heating rate is 968 K. Inconel 718 wrought nickel-chromium alloy was selected for the top face sheet. This has been used for design of ARMOR TPS [3,7]. Inconel 718 has a service temperature of up to 1255 K. For webs, titanium alloys are a suitable material. Ti-6Al-4V alloy was chosen for this preliminary design analysis. The service temperature of this alloy is around 950 K. Even though this is a borderline choice, it is a good material because of its high Young's modulus, high service temperature and low density, which is approximately half that of Inconel.

The bottom face sheet does not need high temperature materials, but it needs to have a high heat capacity. This is because the bottom face sheet acts as a heat sink for the heat conducted into the ITPS. Since the panel is most likely to be attached to the stringers and frames of the vehicle at the bottom face sheet edges, a major portion of the in-plane loads would be borne by the bottom face sheet. Therefore, the material used for bottom face sheet should also have a high Young's modulus. For this purpose a search was performed in the ASM material properties database using CES Selector software by Granta Design. This search has been limited to classical materials, too expensive materials (like certain ceramic matrix composites) were not considered in the search. The constraints for the bottom face sheet material considered for this search were the following: low density ($\rho<4500$kg/m^3), service temperature going up to at least 200ºC, acceptable fracture toughness ($K_{Ic}>15$ MPa.m$^{1/2}$). The materials satisfying these constraints were plotted in the Specific Heat – Young's Modulus plane as shown in Figure 14.

The best material for the bottom face sheet would be in the upper right corner of Figure 14, having a high specific heat as well as a high Young's modulus. The Ti-alloys are in the upper left corner of the plot. There are many materials satisfying the imposed constraints and having higher specific heat than the Ti-alloy. The Young's modulus is lower than that of Ti-alloys for these materials, but wrought aluminum alloys have almost double the

heat capacity of Ti-alloys while at the same time having only a slightly lower Young's modulus. Consequently, Aluminum 2024 alloy was selected for use in the bottom face sheet.
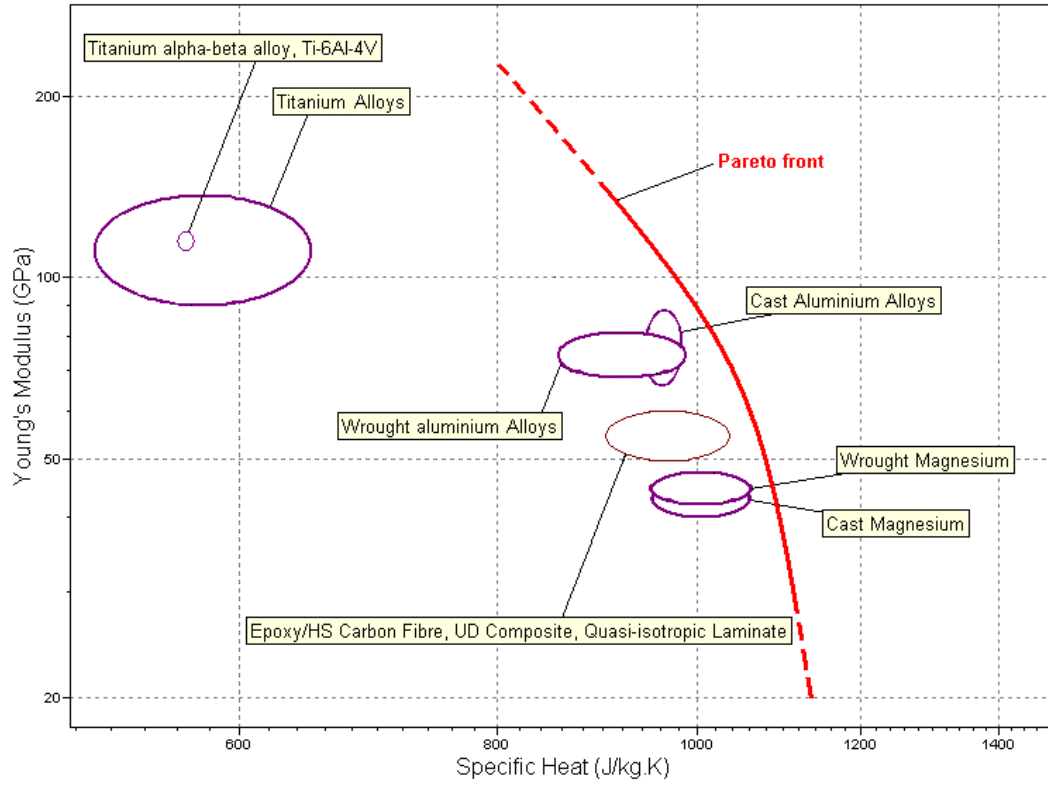
Figure 14. Suitable materials for the bottom face sheet plotted in the Specific Heat –Young's Modulus plane.
Material close to the Pareto front would be most suitable for bottom face sheet.

The ranges chosen for the variable values for preliminary design are listed in Table 2. These ranges were found suitable after a carrying out a few approximate optimization processes. Number of experiments, *N*, used for this preliminary optimization process was 150. The ITPS Optimizer obtained 150 random combinations of variables within their respective ranges and carried out the heat transfer and buckling analyses for each of these combinations to obtain the temperatures and buckling eigen values.

In some cases, the first 40 buckling eigen values may not contain a particular case of buckling. For example, if the bottom face sheet thickness is very high, smallest buckling value for bottom face sheet buckling would be high as well and, therefore, it may not figure among the first 40 eigen values. Thus, there may be a case where there are insufficient number of function evaluations (minimum of 28) to carry out a least squares approximation. In such cases, that particular response surface approximation was discounted under the presumption that the corresponding constraint would not be active in the optimization process. For the 150 experiments in the preliminary design analysis, the number of eigen values obtained from the results file for

t_T	1.0 – 3.0 mm
t_B	3.0 – 8.0 mm
t_W	1.5 – 5.0 mm
θ	79° - 87°
d	80 – 120 mm
p	75 – 150 mm

Table 2. Ranges of the variables chosen from preliminary design.

each buckling case are shown in Table 3. Clearly there are not enough function evaluations to obtain response surfaces for bottom face sheet buckling at Times 1, 2 and 4. At Time 3, the number of values is not sufficient to get

	Time 1	Time 2	Time 3	Time 4
TFS Buckling	127	123	94	123
BFS Buckling	18	21	50	26
Web Buckling	105	98	69	88

Table 3. Number of buckling eigen values for each buckling case. *TFS stands for top face sheet and BFS for bottom face sheet.*

an accurate response surface. Further, it was observed that the bottom face sheet buckling eigen values are available only for cases in which t_B was small (< 2.0 mm). Experience shows that the value of t_B in the optimized design would be much higher than these values. Therefore, the 4 response surfaces for bottom face sheet buckling eigen values were ignored. The total number of response

surfaces was then reduced to 9.

Accuracy of the 9 response surfaces is presented in Table 4. The first response surface referred to by the row header 'Max BFS Temperature' is for maximum bottom face sheet temperature. There are 4 response surfaces for top face sheet buckling referred to as 'TFS Buckling' and 4 response surfaces for web buckling referred to as 'Web Buckling'. The column headers 'Min' and 'Max' stand for minimum and maximum function values used for the response surface calculations, respectively, 'e_{RMS}' stands for root mean square error of the response surfaces approximation and the '% e_{RMS}' stands for percentage of the root mean square error when compared to the average function value. Column header 'e_{PRESS}' stands for PRESS value and '%e_{PRESS}' stands for percentage of PRESS value when compared to the average function value. PRESS is an acronym for Predicted Error Sum of Squares. It is a better indicator of response surface accuracy than the root mean square error.

		Min	Max	e_{RMS}	% e_{RMS}	e_{PRESS}	% e_{PRESS}
Max BFS Temperature		417 K	679 K	0.52 K	0.2	2.08 K	0.9
TFS Buckling	Time 1	0.14	4.55	0.05	3.7	0.13	9.8
	Time 2	0.15	4.58	0.05	3.5	0.11	8.4
	Time 3	0.31	6.77	0.04	2.2	0.12	6.4
	Time 4	0.17	4.87	0.05	3.3	0.11	7.9
Web Buckling	Time 1	0.29	5.02	0.02	1.1	0.05	3.2
	Time 2	0.31	5.96	0.02	1.2	0.08	4.2
	Time 3	0.61	8.16	0.02	0.7	0.05	1.8
	Time 4	0.33	7.16	0.04	2	0.11	5.9

Table 4. Accuracy of temperature and buckling eigen value response surfaces.

The PRESS value is less than 10% in all cases. Therefore, the response surfaces can be viewed as fairly accurate in predicting the smallest buckling eigen values and maximum bottom face sheet temperature. In fact, the temperature response surface has been found to be highly accurate in most cases. It is expected that there will always be a slight error in the buckling response surfaces. The reason for this is that the buckling modes for smallest eigen values could be different for different experiments. For example, the web buckling response surface for the reentry time when the mid point of the web reaches its maximum temperature (Time 4) is determined using 88 function evaluations (Table 3). Even among these 88 values, there were buckling modes which were very different from one another. In some cases the web closest to the panel edge may buckle while in some cases a different web may buckle at the smallest eigen value.

The 9 response surfaces were used for the optimization process, which was carried out using the Matlab function *fmincon*( ). The various optimum designs are presented in Tables 5, 6 and 7. Columns with header 'BFS TempLimit' represent the maximum temperature limit imposed on bottom face sheet and 'Eigen Value Limit' represent the minimum buckling eigen value limit. The next 6 columns give the values of the variables of the optimized designs. The last column is the areal density, *M*, of the optimized design.

The optimized designs in Table 5 were obtained using only the maximum bottom face sheet temperature response surface approximation. Buckling response surfaces were not considered here. This optimization is also known as *thermal sizing*. In these cases, the optimized design had t_T and t_W at the lower bounds while θ, d and p were at their upper bounds. Only t_B changes to accommodate the temperature limit, as shown in Designs 1, 2 and 3. The thermal sizing tends to make the web as thin as possible to reduce the amount of heat coming into the ITPS. The bottom face sheet functions as a thermal mass. This experiment shows that the thermal mass is most effective when put added at the bottom face sheet. This justifies the discussion about the bottom face sheet material selection at the beginning of the section.

	BFS Temp Limit	Eigen value limit	t_T (mm)	t_B (mm)	t_W (mm)	θ (deg)	d (mm)	p (mm)	M (lb/ft^2)
Design 1	150°C	-	1.0	4.8	1.5	87	120	150	4.8
Design 2	180°C	-	1.0	3.6	1.5	87	120	150	4.1
Design 3	200°C	-	1.0	3.0	1.5	87	120	149.1	3.8

Table 5. Thermal sizing designs. *Only the temperature constraint is considered in these designs.*

The designs in Table 6 are obtained by imposing only the buckling constraints and no temperature constraint. The value of t_B is at its lower bound because the bottom face sheet does not experience as huge a temperature rise as the top face sheet and the webs. The values of t_T and t_W increase with increasing buckling eigen value limit. θ is at the upper bound while d and p are at their lower bounds. The buckling optimization tends to drive the ITPS design so that the length of the unsupported sections is as small as possible.

	BFS Temp Limit	Eigen value limit	t_T (mm)	t_B (mm)	t_W (mm)	θ (deg)	d (mm)	p (mm)	M (lb/ft^2)
Design 4	-	1.0	1.1	3.0	1.5	87	80	75	3.8
Design 5	-	1.25	1.2	3.0	1.7	87	80	75	4.0
Design 6	-	1.5	1.4	3.0	1.8	87	80	75	4.2

Table 6. ITPS design with buckling constraints and no temperature constraint.

The designs shown in Table 7 are obtained by imposing both temperature and buckling constraints. These designs are heavier than the previous designs. The reason for this increase can be explained as follows. The temperature constraint drives the value of *d* to the upper bound. In order to increase the buckling resistance of these long sections of webs, the value of t_W is increased. This causes more heat to be conducted into the panel and thus the thermal mass needs to be increased. This is done by increasing the value of t_B. The value of *p* would preferably stay at the upper bound to minimize the areal density. But if the buckling eigen limit is increased, this value decreases in order to decrease the length of the unsupported sections. The stresses built up in the top face sheet are due to the constraining forces exerted by the webs. As these constraining forces change with web thickness and length, the value of t_T adjusts accordingly.

	BFS Temp Limit	Eigen value limit	t_T (mm)	t_B (mm)	t_W (mm)	θ (deg)	d (mm)	p (mm)	M (lb/ft^2)
Design 7	180°C	1.0	2.2	5.2	2.8	87	120	150	7.2
Design 8	180°C	1.25	2.3	6.2	3.3	87	120	132	8.0
Design 9	200°C	1.0	2.0	4.1	2.5	87	120	150	6.2
Design 10	200°C	1.25	2.1	5.3	3.1	87	120	117	7.0

Table 7. Preliminary ITPS designs with bottom face sheet temperature and buckling constraints.

		Design 7		Design 9	
		Predicted	Actual	Predicted	Actual
Max BFS Temperature		180°C	179°C	200°C	198°C
TFS Buckling	Time 1	1.0	1.03	1.0	0.96
	Time 2	1.18	1.20	1.14	1.12
	Time 3	2.44	-	2.08	-
	Time 4	1.33	1.36	1.27	1.25
Web Buckling	Time 1	1.0	1.02	1.0	0.95
	Time 2	1.22	1.18	1.26	1.13
	Time 3	2.08	2.11	1.66	1.68
	Time 4	1.41	1.38	1.44	1.30

Table 8. Comparison of predicted temperatures and buckling values with actual FE values. *There are two blanks in the "Time 3" row of the TFS Buckling because these eigen values do not figure among the first 40 smallest eigen values.*

The geometric variables of Designs 7 and 9 were input into the ITPS Optimizer and the actual finite element temperature and buckling values were obtained. Comparison of the predicted and actual values is shown in Table 8. The generally good agreement shows that the response surface approximations are fairly accurate and the optimization results can be relied upon. As discussed above, ignoring the bottom face sheet buckling response surface does not lead to any constraint violations as the bottom face sheet buckling values are all much greater than unity. The accuracy of the response surfaces can be improved in 2 ways: a) increasing the number of experiments, b) decreasing the range of the variables. A good practice to obtaining an accurate design is to carry out the optimization over a large range and obtain approximate designs by imposing constraints as shown in Table 7. The designs furnish a good range for each variable. The bounds of the variables can then been narrowed down around the approximate designs and new optimization can be carried out to obtain a more accurate design.

Finite element buckling analysis was carried out on Designs 7 and 8 to determine the amount of in-plane loads these designs can withstand. The in-plane loads were imposed along with the aerodynamic pressure load as shown in Figure 15. This is similar to the ascent loading case for an ITPS panel at $x = 827$ inches, the heating rate is almost negligible while there are significant inertia loads. An in-plane load of 10000 N/m was applied on the FE model. The smallest buckling eigen value obtained for Design 7 was 215 and that for Design 8 was 448. This implies that the two designs can withstand in-plane loads up to 2.15×10^6 N/m (12,200 lb/in) and 4.48×10^6 N/m (25,600 lb/in), respectively. However, failure in this case would not be due to buckling but due to yielding. The yield stress for Aluminum 2024 at 200 °C is 260 MPa which would correspond to an in-plane load of approximately 1.35×10^6 N/m (7,720 lb/in). Typical maximum in-plane load for an X-33 like design is approximately 0.29×10^6 N/m (1700 lb/in).
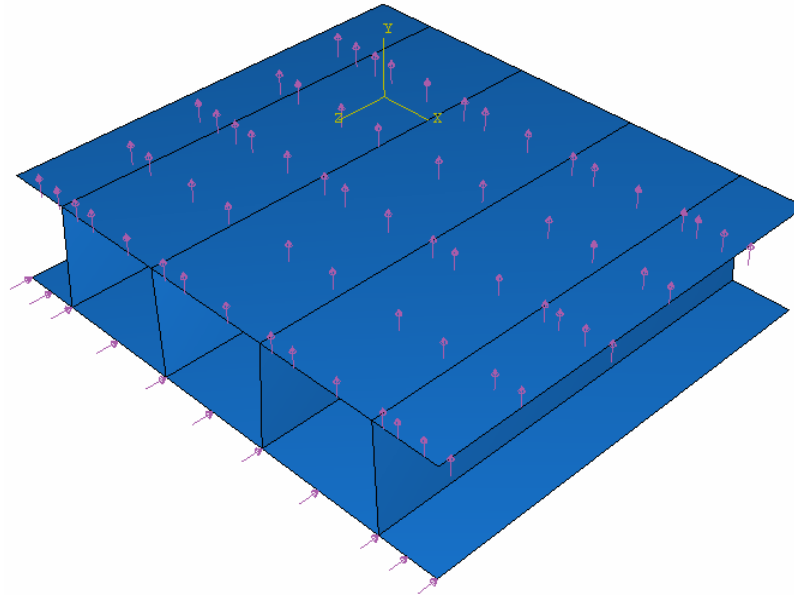
Figure 15. Mechanical loads on the panel during ascent of the vehicle. *The in-plane loads are shown as arrows on the bottom face sheet edge in the front. An aerodynamic pressure load of 1 atm. is applied on the bottom surface of the top face sheet.*

VIII.   Conclusions and Future Work

A procedure has been established for the optimization process aimed at designing a minimum mass integral thermal protection system. The geometry of the corrugated core sandwich panel was simplified and a preliminary design was obtained. Response surface approximation technique used for the optimization process has been found to be very promising and can be used for future design refinements. A flexible Matlab code (ITPS Optimizer) has been developed for generating response surface approximation. This code can be easily altered to accommodate any change in design and material selection. The response surfaces for stresses and top face sheet deflections can also be obtained by the ITPS Optimizer, although this has not been demonstrated in this manuscript.

The optimized mass of the ITPS is around 8 lb/ft². The ARMOR TPS weight for the same heat load is around 2 lb/ft². However, the ARMOR TPS design does not have any provision for in-plane loads and it can take up only light transverse pressure loads. The ITPS, on the other hand, has provisions for both these mechanical loads. It has been demonstrated that the optimized panels could withstand in-plane loads up to 7,700 lb/in. Even while taking this into account, the ITPS areal weight is extremely large. Therefore, the design needs to be drastically altered in order to decrease the weight.

The thermal sizing problem shows that the most effective way to position the thermal mass in the ITPS is at the bottom face sheet. The bottom face sheet also ends up bearing most of the in-plane loads. Therefore, a material with high Young's modulus and high heat capacity should be used for the bottom face sheet. The most effective materials in this category are beryllium alloys. However, beryllium poses many human toxicity risks. In future, optimization studies will be conducted to determine how economical it is to use beryllium alloys for bottom face sheet.

The webs are required to be as thin as possible in order to reduce the ITPS mass as well as the amount of heat entering the ITPS. By decreasing the amount of heat coming into the ITPS, the bottom face sheet thickness and the

height of the sandwich panel can be decreased considerably. Therefore, the material for webs would ideally have a very low conductivity and high Young's modulus. Apart from material selection, the conductivity of the webs can be decreased by removing some material from the webs. This would reduce the total heat conduction path and also reduce the weight of the ITPS. An illustration of this new design is shown in Figure 16. Initial results for temperature and buckling eigen values have been highly encouraging for this design. The buckling eigen values improve, contrary to intuition. The reason behind this could be that there is a decreased resistance to deformation in the webs due to material removal. This decreased resistance leads to lower stresses and thus higher buckling eigen values. One disadvantage of material removal is that the shear stiffness of the sandwich panel reduces considerably.
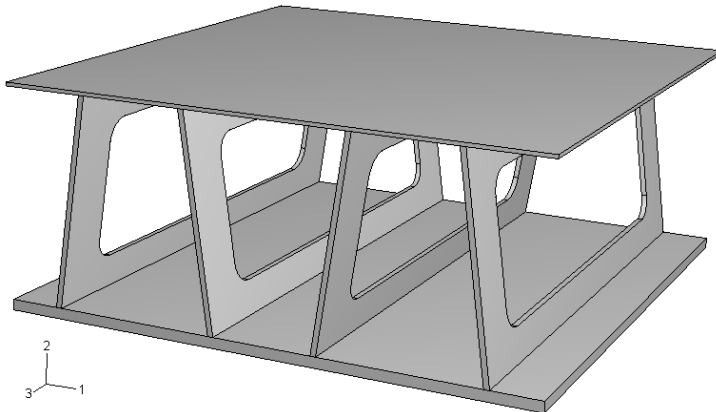
Figure 16. Proposed new design with material removed from the webs.

This could increase the maximum top face sheet deflection as well as bring down the transverse load bearing capacity of the ITPS panel. These two competing factors need to be analyzed. Methods to include these factors in the optimization problem also need to be developed.

Another design alteration to increase the buckling resistance of the webs would be to strategically incorporate stiffeners in the design. Stiffeners increase the buckling resistance without increasing the heat conduction path. The concept of stiffeners can be combined with material removal from the webs to make it more efficient. Stiffeners could also be used in top and bottom face sheet sections. This will help in increasing the length of unit-cells and thus the length of the panel. In the current design, the panel length is reduced because of the buckling constraints. Large ITPS panels would imply smaller number of stringer and frames. This would reduce the overall weight of the skin. However, material removal and introduction of stiffeners would introduce additional variables in the design process. These design changes and the new challenges arising from them will be studied in future.

Acknowledgments

References

[1]Blosser, M. L., "Advanced metallic thermal protections systems for reusable launch vehicles," *Doctoral Dissertation*, Department of Mechanical and Aerospace Engineering, University of Virginia, Charlottesville, VA, May 2000.

[2]Dorsey, J. T., Poteet, C. C., Wurster, K. E., Chen, R. R., "Metallic thermal protection system requirements, environments, and integrated concepts," *Journal of Spacecraft and Rockets*, Vol. 41, No. 2, Mar – Apr 2004, pp. 162-172.

[3]Poteet, C. C., Abu-Khajeel, H., Hsu, S-Y, "Preliminary thermal-mechanical sizing of a metallic thermal protection system," *Journal of Spacecraft and Rockets*, Vol. 41, No. 2, Mar – Apr 2004, pp. 173-182.

[4]Blosser, M. L., "Fundamental modeling and thermal performance issues for metallic thermal protection system concept," *Journal of Spacecraft and Rockets*, Vol. 41, No. 2, Mar – Apr 2004, pp. 195-206.

[5]Zhu, H., Sankar, B. V., Haftka, R. T., Venkataraman, S., Blosser, M. L., "Minimum mass design of insulation made of functionally graded material," *Journal of Spacecraft and Rockets*, Vol. 41, No. 3, May – June 2004, pp. 467-469

[6]Zhu, H., "Design of metallic foams as insulation in thermal protection systems," *Doctoral Dissertation*, Department of Mechanical and Aerospace Engineering, University of Florida, Gainesville, FL, 2004.

[7]Blosser, M.L., Development of Advanced Metallic, Thermal-Protection-System Prototype Hardware, Journal of Spacecraft and Rockets, Vol. 41, No. 2, Mar-Apr 2004, pp.